Direct Form I Realization of Active Photonic Filters

By

Jian Tong, Duncan L. MacFarlane, Issa Panahi, L. Roberts Hunt, Govind Kannan

The Erik Jonsson School of Engineering and Computer Science

The University of Texas at Dallas

Richardson, Texas 75083

jxt021000@utdallas.edu

Gary A. Evans and Marc P. Christensen

Department of Electrical Engineering

Southern Methodist University

Dallas, Texas 75275

Abstract

An integrated photonic architecture is introduced and used to realize an optical filter with direct form I realization. The architecture offers gain from semiconductor optical amplifiers, and this gain results in an active optical filter whose filter response depends on the individual gains. The presence of gain provides advantages in filter performance, and tunable and adaptive functionality. The optical filter is modeled as a discrete time system and the z-transform is used in its analysis and design. A low-pass filter design example is presented and the filter coefficients are derived in terms of gains and coupler splitting ratios. The region of stable operations is derived by applying the Schur-Cohn stability test.

Index Terms: Photonic Filter, z-Transform, semiconductor optical amplifier.

I. Introduction

The photonics community has embraced electrical filter theory and techniques in the design of optical filters [1-12]. All filters, including optical filters, consist of splitters, delays and combiners. Like their electronic counterparts, optical filters are completely described by their frequency response so long as they are linear and time invariant (LTI). Therefore, digital signal processing provides a readily available mathematical framework, the z transform, for the design of optical filters [4, 5]. The fundamental relationships between optical waveguide and filters were developed by Moslehi, Goodman, Tur and Shaw in 1984 [1]. Recently, theoretical and experimental research on optical filter design and analysis based on z-transform techniques allowed the application of DSP algorithms [4, 5, 7, 9-12]. In particular, MacFarlane and Dowling interpreted the multi-stage Fabry-Perot type etalons as discrete time lattice filters, and synthesized filters with desirable properties in 1994 [5]. With their seminal textbook, Madsen and Zhao significantly advanced both the theoretical and experimental research, and brought the formalism into the mainstream of photonics [8].

One lesson from filter theory is that any transfer function may be realized in standard formats, for example, the direct form I realization [13]. This direct form I realization is shown in Fig. 1 using the transform z^{-1} block to represent a unit delay. This unit delay can be interpreted as $T = Ln/c$ in an optical system, where L is the smallest light path length and c/n is the speed of light in material. The rational system function for this, and any LTI filter, is given by

$$H(z) = \frac{\sum_{k=0}^{M} b_k z^{-k}}{1 + \sum_{k=1}^{N} a_k z^{-k}} \tag{1}$$

This general form characterizes an infinite impulse response (IIR) system. Here the *a's* and *b's* in the polynomials are exactly the weights on the branches of the direct form I realization shown in Figure 1. The zeros and poles of the system function depend on the choice of the system parameters *b's* and *a's,* and determine the frequency response characteristics of the system. The direct form I realization system can be viewed as two systems in cascade, that is

$$H(z) = H_z(z)H_p(z) \tag{2}$$

$$H_z(z) = \sum_{k=0}^{M} b_k z^{-k} \tag{3}$$

$$H_p(z) = \frac{1}{1 + \sum_{k=1}^{N} a_k z^{-k}} \tag{4}$$

Here $H_z(z)$ consists of the zeros of $H(z)$, and $H_p(z)$ consists of the poles of $H(z)$. The system stability is completely determined by the properties of $H_p(z)$, which we will discuss later in Section IV. In this paper we show that the direct form I structure can be implemented as a corresponding photonic filter. An advantage of direct form electrical filters is that filter parameters *a's* and *b's* may be directly set or adjusted in the architecture according to the given transfer functions [13]. The same property can be realized by including "gain" elements in photonic structure to create active optical filters. The additional presence of gain provides advantages in filter performance, and tunable and adaptive functionality.

The purpose of this paper is to introduce an integrated photonic architecture in which active optical filters can be realized directly in the direct form I realization. In this architecture, semiconductor optical amplifiers (SOA) are used for providing gains and photonic couplers are used to split and combine the intermediate signals. In Section II we describe the photonic

architecture. In Section III we develop the filter analysis and design techniques. In Section IV we explore the region of stable operation using the Schur-Cohn test.

II. Photonic Architecture

Our filter is constructed using SOAs coupled together by photonic couplers. The SOA sections provide the weights and the delays that describe any filter. The inclusion of gain given by SOAs makes this an active photonic filter architecture. The presence of gain provides a tunable filter and adaptive functionality that also enables the direct form I filter structure as shown in Figure 1 to be implemented. In Figure 2 is shown a top view schematic of the active photonic filter that uses semiconductor laser amplifiers to provide gains and delays. By way of example, the figure shows a 3rd order direct form I realization active photonic filter. The filter stage gain is controlled by the injection current to the individually addressable gains in the SOA active regions. These regions also provide the phase delays that lead to filter responses. Also on the surface of the substrate are photonic couplers that can split and combine optical signals.

The device is fabricated using a multiple quantum well (MQW) epitaxial growth with ridge waveguide processing. The active region consists of 5x85Å compressively strained AlInGaAs quantum wells, which are designed for 1550nm wavelength operation and provide gain for TE polarized light. Patterned p-type electrodes facilitate individual addressing of the SOA gates. The ridge waveguide formed with reactive ion etching (RIE) is 2.5um wide and 1.3 um high, which supports single transverse mode operation. After cleaving, the device is antireflection coated to less than 1% reflectivity.

At the junctions of the semiconductor amplifying sections photonic couplers were machined in order to split the signal into equal components. These total internal reflection (TIR) mirror couplers were designed using Finite Difference Time Domain modeling software, and the

parameters that were optimized included the angle of the facet, the size, and location. A contour plot of the numerical results is shown in Fig. 3. The TIR mirrors are fabricated in a two-step procedure using focused ion beam (FIB) micromachining. A 4um deep trench is first directly milled, and cross session cleaning is then applied to remove the redeposition during FIB milling process. An SEM of the obtained TIR mirror as shown in Fig. 4 is optically smooth and the sidewall angle is less than 1 degree.

In operation, an optical signal is injected into the heterojunction of the structure where it undergoes gain and delay. At the photonic couplers the signal is split or combined. With the advantage of adjustable gains, active optical filters offer a more flexible approach to yield desired system response. Furthermore, the adjustable gains provide a degree of programmability to the optical filter to great economic advantage: the same structure can be fabricated to support different user designated applications.

III. Filter analysis and design

An attractive feature of the Direct Form I realization photonic filter is the direct relationship between the gains and the designed filter transfer function. The active photonic filter structure shown in Figure 2 can be completely described by the block diagram format as shown in Figure 5. Gain variables can be set to match the weights of each signal branch of the direct form I structure as shown in Figure 1. The fixed-length waveguide confined to gain region provides phase delay, $z^{-1/2}$, for filter system. The transfer function of all-zero system shown in Figure 5 can be derived in terms of couplers splitting ratios (ρ, τ) and gains (G) as following expression,

$$H_z(z) = b_0 z^{-1} + b_1 z^{-2} + b_2 z^{-3} + b_3 z^{-4} = z^{-1}(b_0 + b_1 z^{-1} + b_2 z^{-2} + b_3 z^{-3}) \quad (5)$$

where

$$b_0 = \tau_{0,0} G_{1,0} \tau_{2,0} G_{3,0} \tag{6}$$

$$b_1 = \rho_{0,0} G_{0,1} \rho_{0,2} G_{1,2} \rho_{2,2} G_{2,1} \rho_{2,0} G_{3,0} \tag{7}$$

$$b_2 = \rho_{0,0} G_{0,1} \tau_{0,2} G_{0,3} \rho_{0,4} G_{1,4} \rho_{2,4} G_{2,3} \tau_{2,2} G_{2,1} \rho_{2,0} G_{3,0} \tag{8}$$

$$b_3 = \rho_{0,0} G_{0,1} \tau_{0,2} G_{0,3} \tau_{0,4} G_{0,5} \rho_{0,6} G_{1,6} \rho_{2,6} G_{2,5} \tau_{2,4} G_{2,3} \tau_{2,2} G_{2,1} \rho_{2,0} G_{3,0} \tag{9}$$

Similarly, the transfer function for all-pole system is given as,

$$H_p(z) = \frac{kz^{-1}}{1 + a_1 z^{-1} + a_2 z^{-2} + a_3 z^{-3}} \tag{10}$$

where

$$k = \tau_{4,0} G_{5,0} \tau_{6,0} G_{7,0} \tag{11}$$

$$a_1 = 0 \tag{12}$$

$$a_2 = -\rho_{6,0} G_{6,1} \rho_{6,2} G_{5,2} \rho_{4,2} G_{4,1} \rho_{4,0} G_{5,0} \tag{13}$$

$$a_3 = -\rho_{6,0} G_{6,1} \tau_{6,2} G_{6,3} \rho_{6,4} G_{5,4} \rho_{4,4} G_{4,3} \tau_{4,2} G_{4,1} \rho_{4,0} G_{5,0} \tag{14}$$

Because of the orientation of the photonic delays, a_1 equals to *0* for any order photonic filter system discussed in this paper. The system shown in Figure 5 can also be viewed as two systems in cascade, that is,

$$H(z) = H_z(z)H_p(z) \tag{15}$$

By substituting equation (5) and (10) into (15) we obtain,

$$H(z) = \frac{(b_0 + b_1 z^{-1} + b_2 z^{-2} + b_3 z^{-3})kz^{-2}}{1 + a_2 z^{-2} + a_3 z^{-3}} \tag{16}$$

The constant k is an overall amplification coefficient, and the extra z^{-2} in the numerator gives only pure phase delay and does not affect system magnitude response. The constant k and the extra z^{-2} are neglected in the following filter response analysis. Consequently, the system response of the shown photonic filter is determined by parameters *a's* and *b's* which are exactly the weights of direct form I realization filter structure (except a_1 equals to *0*). To simplify the analysis, we assume photonic coupler is lossless ($\rho^2+\tau^2 =1$) and its splitting ratio to be equal to 3 dB. The coupler's reflection coefficient (ρ) is negative while the transmission coefficient (τ) is positive. All the gains discussed in this paper are positive.

As a first example, we begin with a passive filter structure by setting all the gains in a 3rd order system equal to 1. This results in the transfer function

$$H(z) = \frac{0.5 + 0.25z^{-1} + 0.125z^{-2} + 0.0625z^{-3}}{1 - 0.25z^{-2} - 0.125z^{-3}} \tag{17}$$

The magnitude and phase response of the filter is shown in Figure 6. The passband of the given filter is located at low frequency, as the dominant pole is sitting on real axis as shown in Figure 7.

In optical communication system, bandpass filters with high quality factor (Q) raise more interests in applications such as wavelength division multiplexing (WDM) channels demulitplexing. Q factor is a measure of the sharpness or selectivity of the filter defined by

$$Q = \frac{v_0}{\Delta v_{1/2}} \tag{18}$$

Where v_0 is the peak frequency and $\Delta v_{1/2}$ is the Full Width at Half of the Maximum (FWHM). One of the advantages of the active photonic filter is the inclusion of gains which enables us to adjust filter parameters to obtain desired frequency response. The value of each gain of the photonic filter structure is given in Table 1 for a third order system. $G_{1,0}$, $G_{1,2}$, $G_{1,4}$, $G_{1,6}$, $G_{5,2}$, and $G_{5,4}$ are used for setting transfer function parameters *a's* or *b's*. The other gain elements are set here to compensate split signal intensity at the photonic couplers, because at the branching node of digital signal processing systems, the intensity of each of the output signals equals to the input signal. High Q value can be achieved by forcing the dominant poles moving toward unit circle for the given 3rd order filter system. The transfer function is given as,

$$H(z) = \frac{1 + 0.1z^{-1} + 0.05z^{-2} + 0.1z^{-3}}{1 - 0.5z^{-2} - 0.49z^{-3}} \tag{19}$$

System response and zero-pole distributions are shown in Figure 8 and 9 respectively. The design is straightforward. As the system response as well as transfer function were given, we may substitute those filter parameters *a's* and *b's* into Table 1 and find the corresponding gains values for $G_{1,0}$, $G_{1,2}$, $G_{1,4}$, $G_{1,6}$, $G_{5,2}$, and $G_{5,4}$. The results are shown in Table 2. In considering the example of Eqs (17) and (19) it is important to note that the user applied gains control the filter response, and that the same device may be used in both cases.

IV. Stability

In the above example we started with a stable filter and implemented the transfer function in a manner that maintains stability. In general it is desirable to explicitly understand and control

the stability for the filter. For all filters, stability is described by the denominator and in particular the roots of the denominator *A(z)*, or poles. For a causal LTI system, all the poles must lie inside the unit circle for the system to ensure stability. There are several stability criteria that aid us to determine if any of the roots of *A(z)* lies outside the unit circle. The Schur-Cohn stability test [13] is used here to derive the constraints on the gain values securing stability of the above filter.

The Schur-Cohn stability test states that the polynomial *A(z)* has all its roots inside the unit circle if and only if the coefficients K_m satisfy the condition $|K_m|<1$ for all $m=1,2,..N$. where K_m can be calculated using the following equations (20) through (23).

$$A_m(z) = \sum_{k=0}^{m} a_m(k) z^{-k} \tag{20}$$

$$B_m(z) = z^{-m} A_m(z^{-1}) \tag{21}$$

$$A_{m-1}(z) = \frac{A_m(z) - K_m B_m(z)}{1 - K_m^2} \tag{22}$$

$$K_m = a_m(m) \tag{23}$$

For the 3rd order filter in the previous example, applying Schur-Cohn stability test yields,

$$|K_3| = |a_3| < 1 \tag{24}$$

$$|K_2| = \left| \frac{a_2}{1 - a_3^2} \right| < 1 \tag{25}$$

$$|K_1| = \left| \frac{a_2 a_3}{1 - a_3^2 + a_2} \right| < 1 \tag{26}$$

Since a_2 and a_3 are negative as shown in equation (13) and (14), using equation (24), (25) and (26) we obtain,

$$0 > a_2 - a_3^2 > -1 \tag{27}$$

$$0 > a_2 + a_3 > -1 \tag{28}$$

Equation (28) puts a more restrictive limit on a_2 and a_3 than equation (27) does, because a_3 is negative and also bounded by equation (24).

Upon substituting equations (13) and (14) into equations (24) and (28), the filter stability in terms of coupler splitting ratios and SOAs gains is given as,

$$\rho_{6,0} G_{6,1} \tau_{6,2} G_{6,3} \rho_{6,4} G_{5,4} \rho_{4,4} G_{4,3} \tau_{4,2} G_{4,1} \rho_{4,0} G_{5,0} < 1 \tag{29}$$

$$\rho_{6,0} G_{6,1} \rho_{6,2} G_{5,2} \rho_{4,2} G_{4,1} \rho_{4,0} G_{5,0} + \rho_{6,0} G_{6,1} \tau_{6,2} G_{6,3} \rho_{6,4} G_{5,4} \rho_{4,4} G_{4,3} \tau_{4,2} G_{4,1} \rho_{4,0} G_{5,0} < 1 \tag{30}$$

If we fix, for example, all coupler splitting ratios to be the same 50% reflection and 50% transmission ($\rho = -\frac{1}{\sqrt{2}}, \tau = \frac{1}{\sqrt{2}}$), applying Table 1 the stability results simply to

$$G_{5,4} < \sqrt{2} \tag{31}$$

$$G_{5,2} + G_{5,4} < \sqrt{2} \tag{32}$$

where filter stability is maintained. For higher order filter systems, the calculation complexity of Schur-Cohn stability test increases, other methods may apply to evaluate the stability [12].

V. Conclusion

In this paper, we introduced an integrated photonic architecture in which active optical filters could be realized directly in the Direct form I realization. The optical filter design and analysis was based on traditional filter theory and the system response of a 3rd order filter structure was demonstrated. Design parameters and gains were calculated to generate required filter transfer function. Filter stability was discussed and the region for gain values was derived by applying Schur-Cohn stability test. Taken in the context of recent optical filter theory, this work provided an example of a new photonic filter realization for a traditional electrical form. More fundamentally, this paper also illustrated the use of gain in optical filters to improve quality factor and to provide a degree of programmability.

This structure is flexible and programmable. The order of filter block can be easily expanded because of the repeatable structure, and gains can be set to yield desired filter parameters for required application. The form of filter that can be realized with a particular arrangement of delay stages, with or without gain, depends on the availability and selection of coupler. In this case, we have shown that a simple coupler may be used to realize a direct form 1 realization. Lattice filters, and more complicated structures will follow from other types of couplers.

As would be expected from a simple textbook example, there are some limitations of the obtained transfer function. Because of the specific orientation of the photonic delays, the a_1 is always set to be zero. As a result, sum of the poles is equal to zero. This leads to restriction on the poles. Many desired transfer functions will have to be approximated and implemented by

higher order filters than prescribed. Also in line with the optical architecture we have limited the discussion to positive gains. As a result, all *b's* in the numerator are positive, while all *a's* in the denominator are negative as indicated in Table 1. As in traditional filter theory there are different photonic realizations, including lattice filters and feed forward filters, to provide different performance strengths. In all of these realizations the addition of gain will provide interesting and useful behaviors.

References

[1] B. Moslehi, J. W. Goodman, M. Tur and H. J. Shaw, "Fiber optic lattice signal processing," *Proceedings of the IEEE*, 72, 909-930 (1984).

[2] F. J. Fraile-Peláez, J. Capmany, and M. A. Muriel, "Transmission bistability in a double-coupler fiber ring resonator," *Optics Letters*, Vol. 16, No. 12, 907-909 (1991).

[3] K. Sasayama, M. Okuno, and K. Habara, "Coherent optical transversal filter using silica-based waveguides for high-speed signal processing," *J. Lightw. Technol.*, vol. 9, no. 10, pp. 1225-1230, 1991.

[4] D. L. MacFarlane and E. M. Dowling, "Z-domain techniques in the analysis of Fabry-Perot etalons and multilayer structures," *J. Opt. Soc. Am. A*, 11, 236-245 (1994).

[5] E. M. Dowling and D. L. MacFarlane, "Lightwave lattice filters for optically multiplexed communication systems," *J. Lightwave Technology* 12, 471-486 (1994).

[6] Y. Li, C. Henry, E. Laskowski, C. Mak, and H. Yaffe, "Waveguide EDFA gain equalization filter," *Electron. Lett.*, vol. 31, no. 23, pp. 2005-2006, 1995.

[7] D. L. MacFarlane, E. M. Dowling, and V. Narayan, "Ring resonators with NxM couplers," *Fiber and Integrated Optics* 14, 195-210 (1995).

[8] C. Madsen and J. Zhao, *Optical Filter Design and Analysis: A Signal Processing Approach,* New York, NY: John Wiley, 1999.

[9] Duncan L. MacFarlane, Jian Tong, Chintan Fafadia, Vishnupriya Govindan, L. Roberts Hunt, and Issa Panahi "Extended Lattice Filters Enabled by Four Directional Couplers" Applied Optics Vol. 43, No. 33, pp6124-6133, Nov 2004

[10] Duncan MacFarlane, Jian Tong, L. Roberts Hunt, Issa Panahi, Tiberiu Constantinescu, V. Ramakrishna, Gary Evans and Marc Christensen, "Active Optical Lattice FIlters," 2005 IEEE

LEOS Summer Topicals: Optical Signal Processing Theory, Technologies and Application San Diego, California, July 25-27, 2005 (Invited)

[11] L. Roberts Hunt, Vishnupriya Govindan, Issa Panahi, Jian Tong, Govind Kannan and Duncan L. MacFarlane, "Active Optical Lattice Filters" EURASIP Journal on Applied Signal Processing 2005:10, pp1452-1461 (2005)

[12] Issa Panahi, Govind Kannan, L. Roberts. Hunt, Duncan. L. MacFarlane, Jian Tong, "Lattice filter with adjustable gains and its application in optical signal processing," IEEE Statistical Signal Processing Workshop, Bordeaux, France, July 17-20, 2005

[13] J. Proakis and D. Manolakis, *Digital Signal Processing Principles, Algorithms, and Applications,* New Jersey, Prentice-Hall, 1996

Figure Captions

1 Figure 1. Block diagram for direct form I realization.

2 Figure 2. Schematic of the active photonic filter architecture

3 Figure 3. Finite Different Time Domain theoretical design of a TIR mirror coupler showing a preferred position for equal splitting of an input signal.

4 Figure 4. Scanning Electron Microscope image of a TIR mirror waveguide splitter with totally internally reflecting mirror.

5 Figure 5. Integrated beam-splitter fabricated by focused-ion beam etching

6 Figure 6. Block diagram for the active photonic filter architecture shown in Figure 2

7 Figure 7. Magnitude and phase response of the filter of which transfer function is given as equation (17)

8 Figure 8. Zeros and poles of system response of the filter of which transfer function is given as equation (17)

9 Figure 9. Magnitude and phase response of the filter of which transfer function is given as equation (19)

10 Figure 10. Zeros and poles of system response of the filter of which transfer function is given as equation (19)

Figure 1

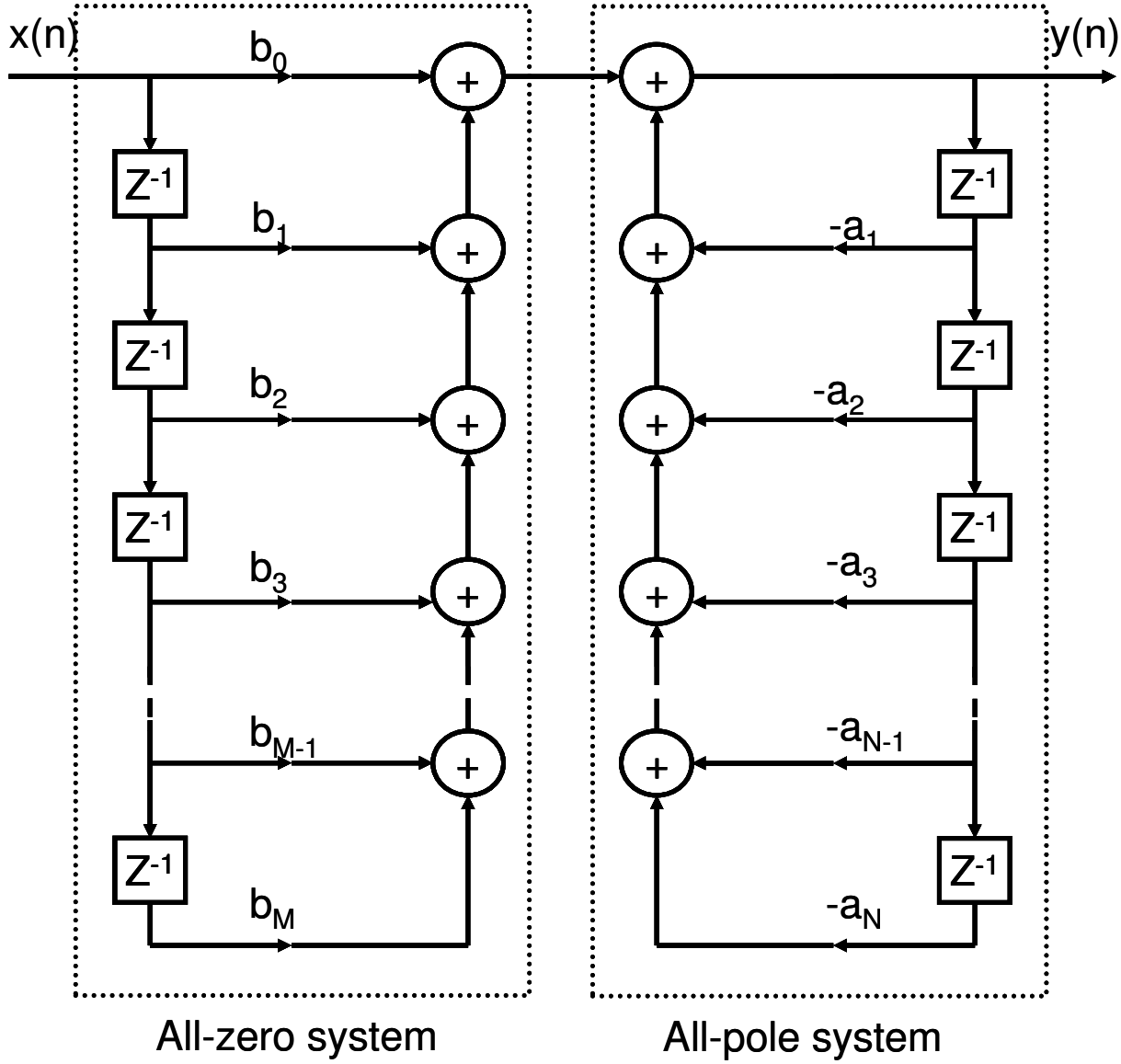
x(n)
y(n)
b0
b1
b2
b3
bM-1
bM
-a1
-a2
-a3
-aN-1
-aN
Z-1
All-zero system
All-pole system

Figure 2

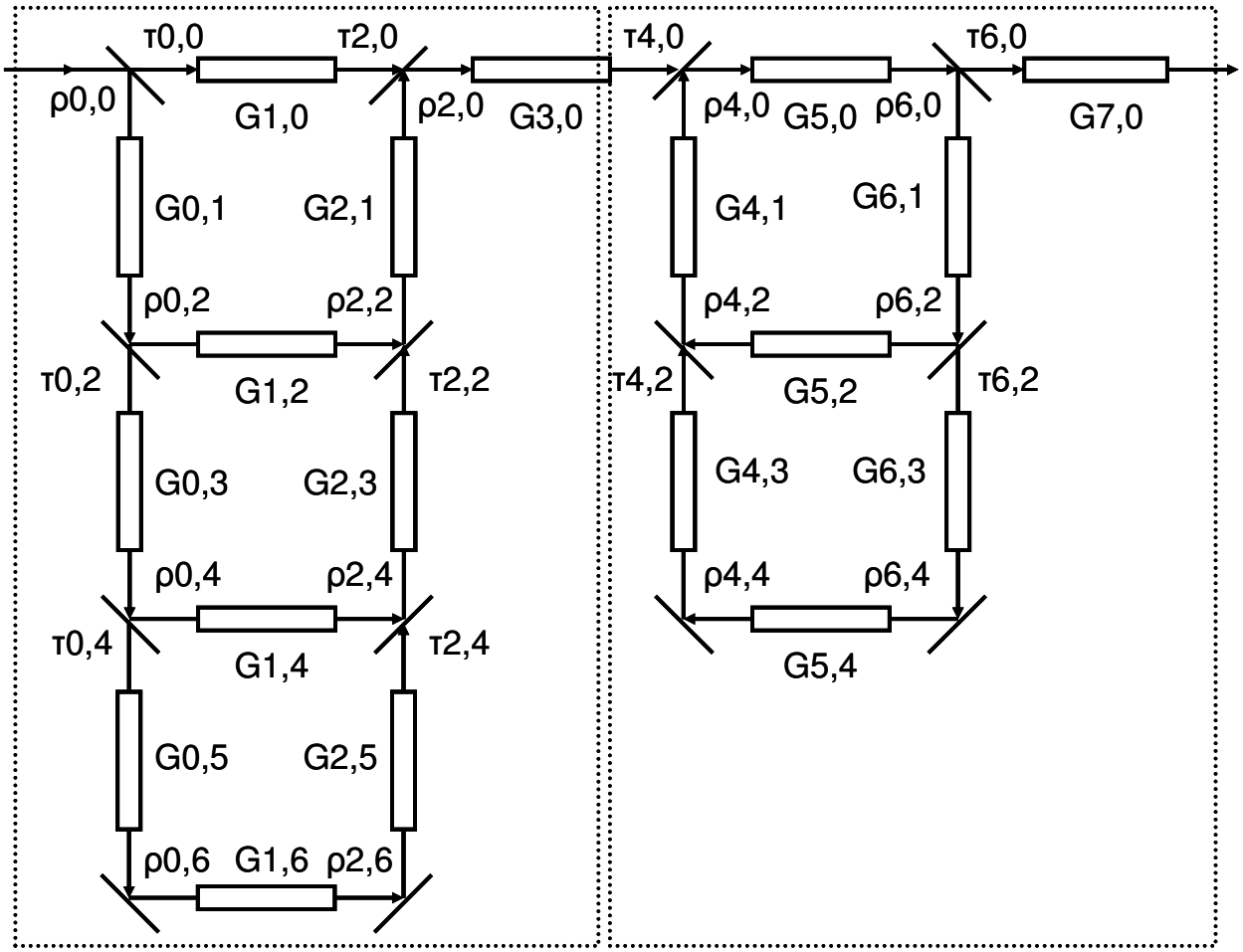
τ0,0
τ2,0
τ4,0
τ6,0
ρ0,0
G1,0
ρ2,0
G3,0
ρ4,0
G5,0
ρ6,0
G7,0
G0,1
G2,1
G4,1
G6,1
ρ0,2
ρ2,2
ρ4,2
ρ6,2
τ0,2
G1,2
τ2,2
τ4,2
G5,2
τ6,2
G0,3
G2,3
G4,3
G6,3
ρ0,4
ρ2,4
ρ4,4
ρ6,4
τ0,4
G1,4
τ2,4
G5,4
G0,5
G2,5
ρ0,6
G1,6
ρ2,6

Figure 3

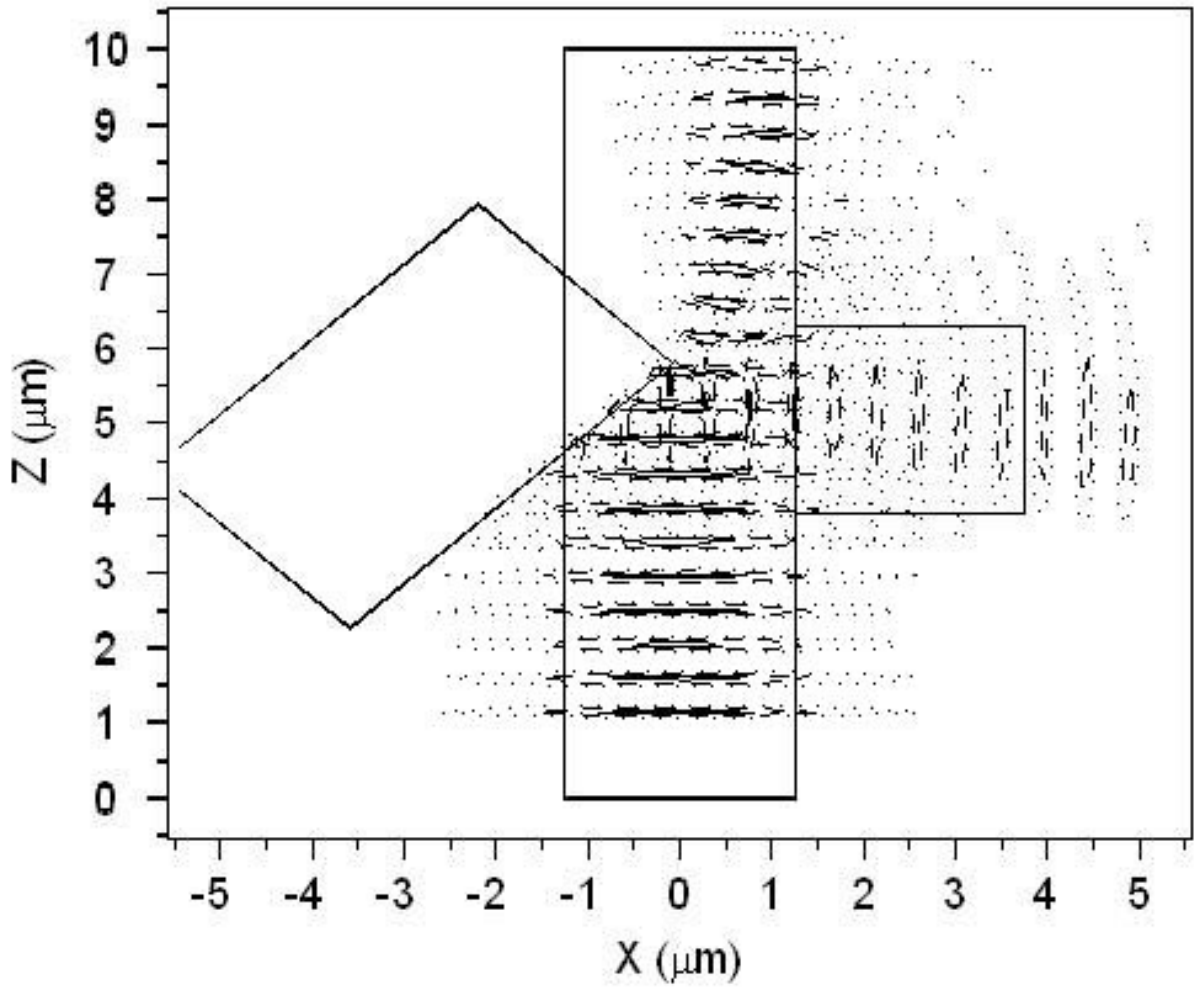

Figure 4

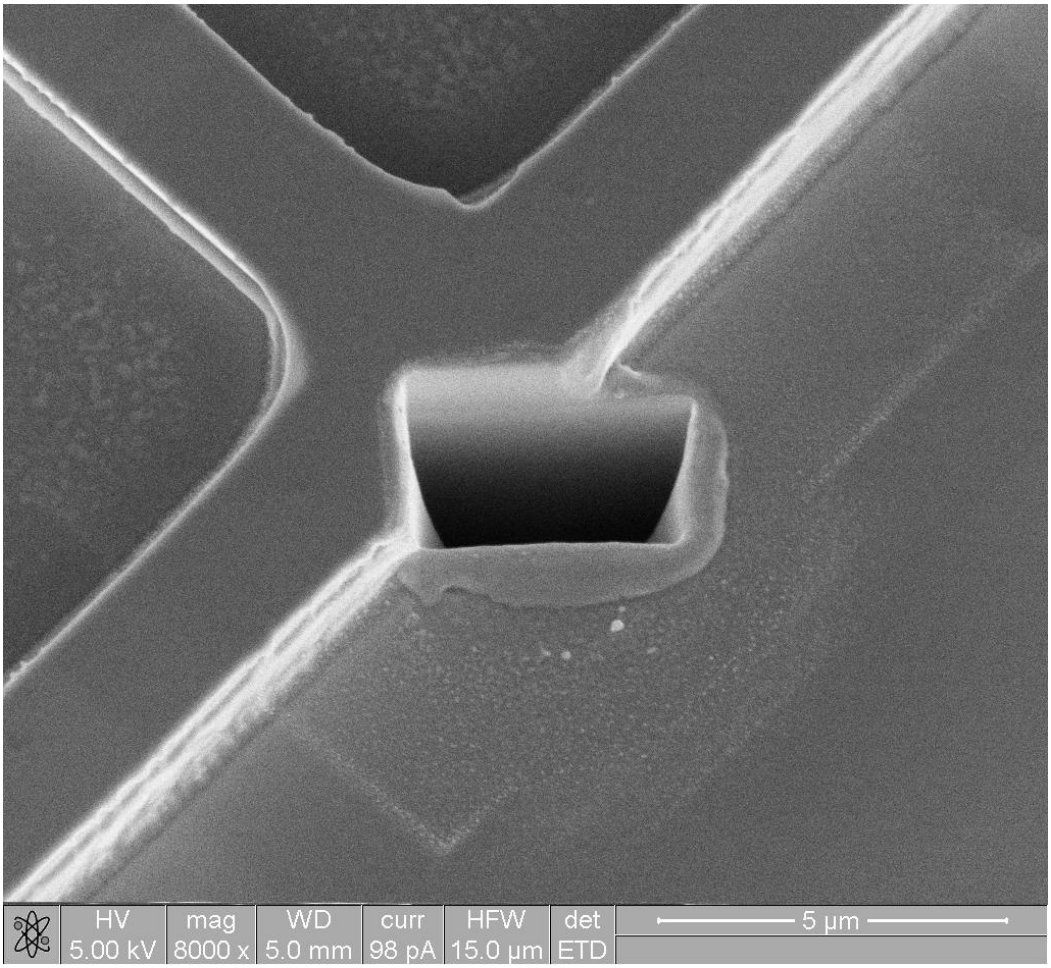

Figure 5

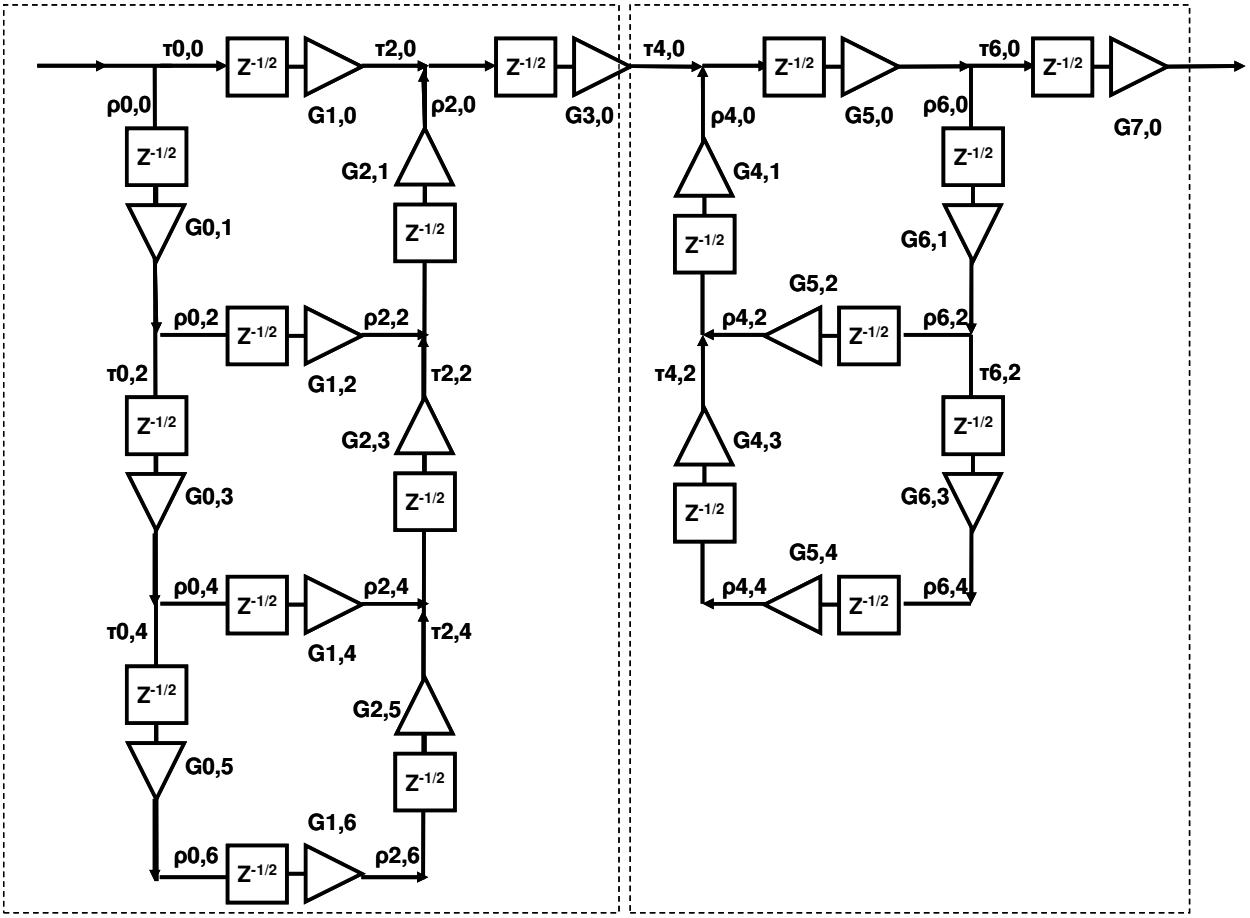
τ0,0
Z-1/2
τ2,0
Z-1/2
τ4,0
Z-1/2
τ6,0
Z-1/2
ρ0,0
G1,0
ρ2,0
G3,0
ρ4,0
G5,0
ρ6,0
G7,0
Z-1/2
G2,1
G4,1
Z-1/2
G0,1
Z-1/2
G6,1
G5,2
ρ0,2
Z-1/2
ρ2,2
ρ4,2
Z-1/2
ρ6,2
τ0,2
G1,2
τ2,2
τ4,2
τ6,2
Z-1/2
G2,3
G4,3
Z-1/2
G0,3
Z-1/2
G6,3
G5,4
ρ0,4
Z-1/2
ρ2,4
ρ4,4
Z-1/2
ρ6,4
τ0,4
G1,4
τ2,4
Z-1/2
G2,5
G0,5
Z-1/2
G1,6
ρ0,6
Z-1/2
ρ2,6

Figure 6

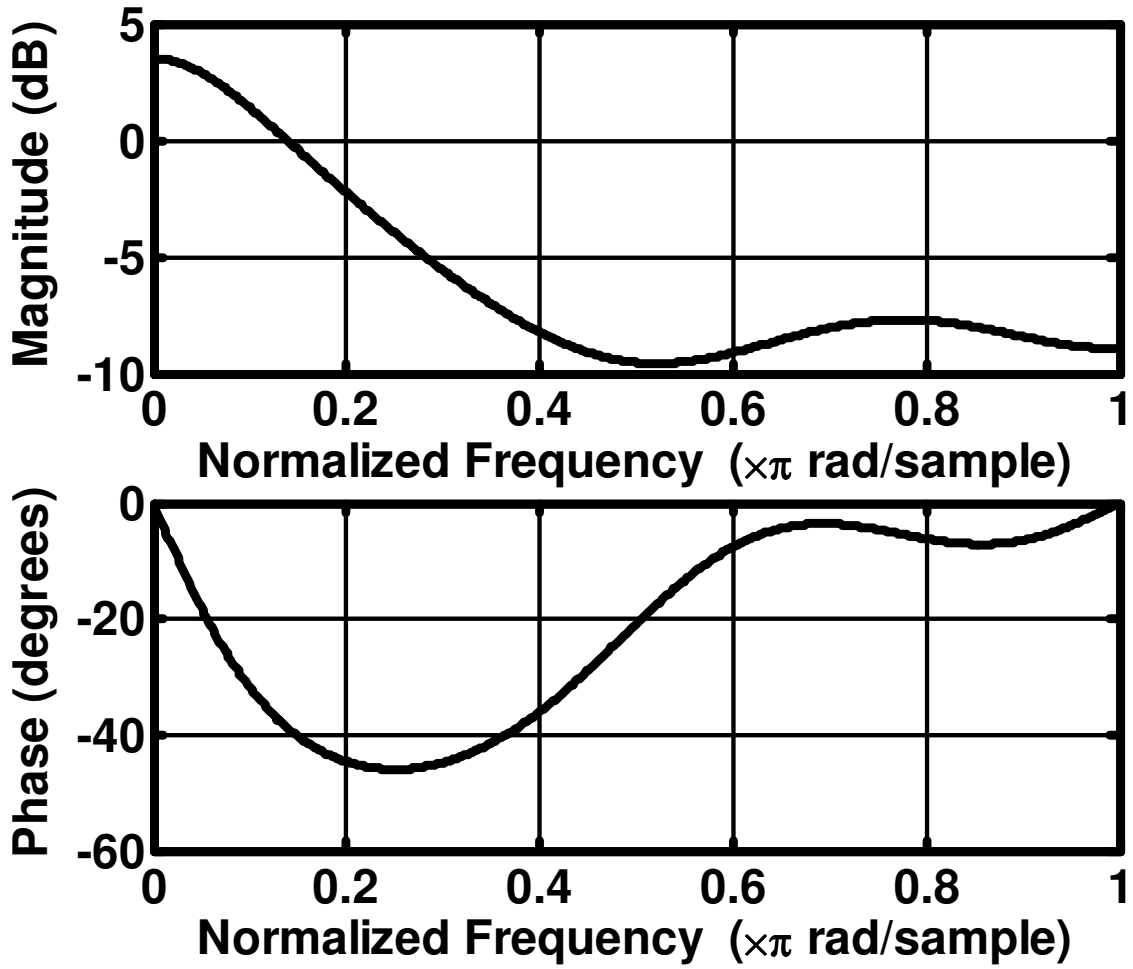
Magnitude (dB)
5
0
-5
-10
0
0.2
0.4
0.6
0.8
1
Normalized Frequency (×π rad/sample)
Phase (degrees)
0
-20
-40
-60
0
0.2
0.4
0.6
0.8
1
Normalized Frequency (×π rad/sample)

Figure 7

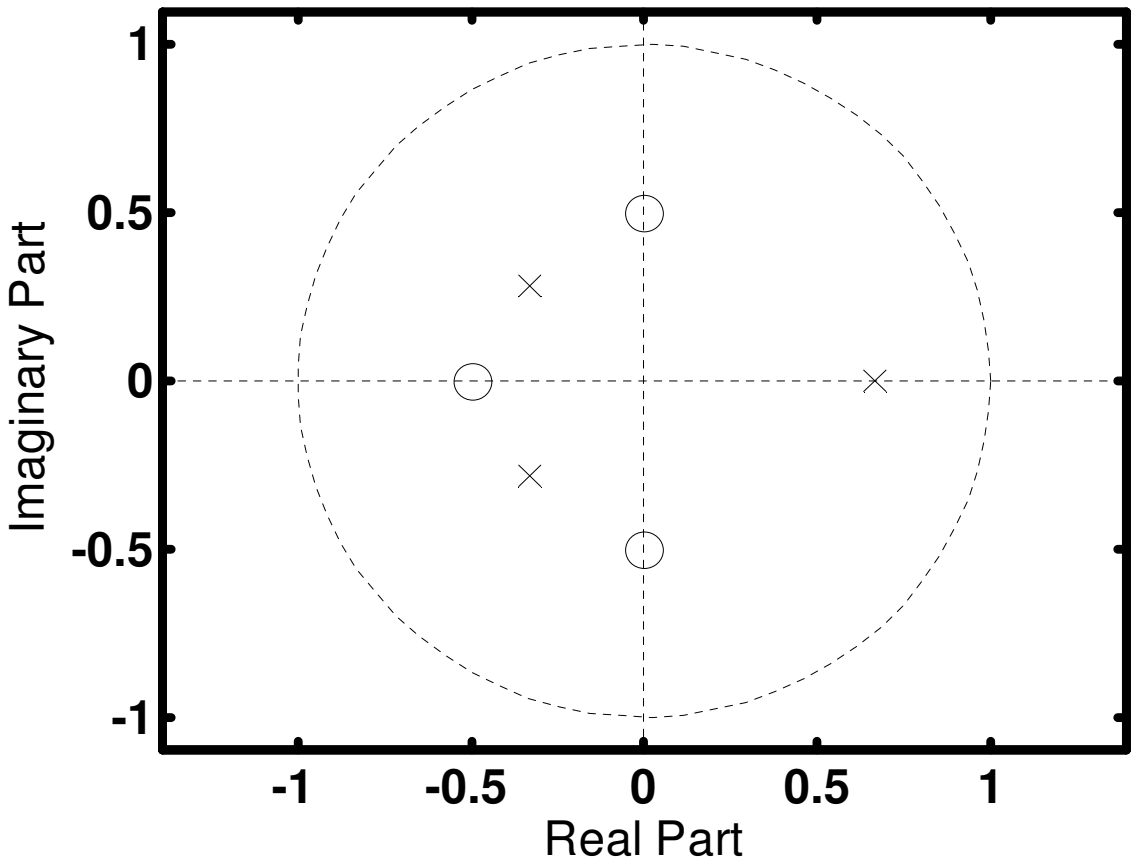

Figure 8

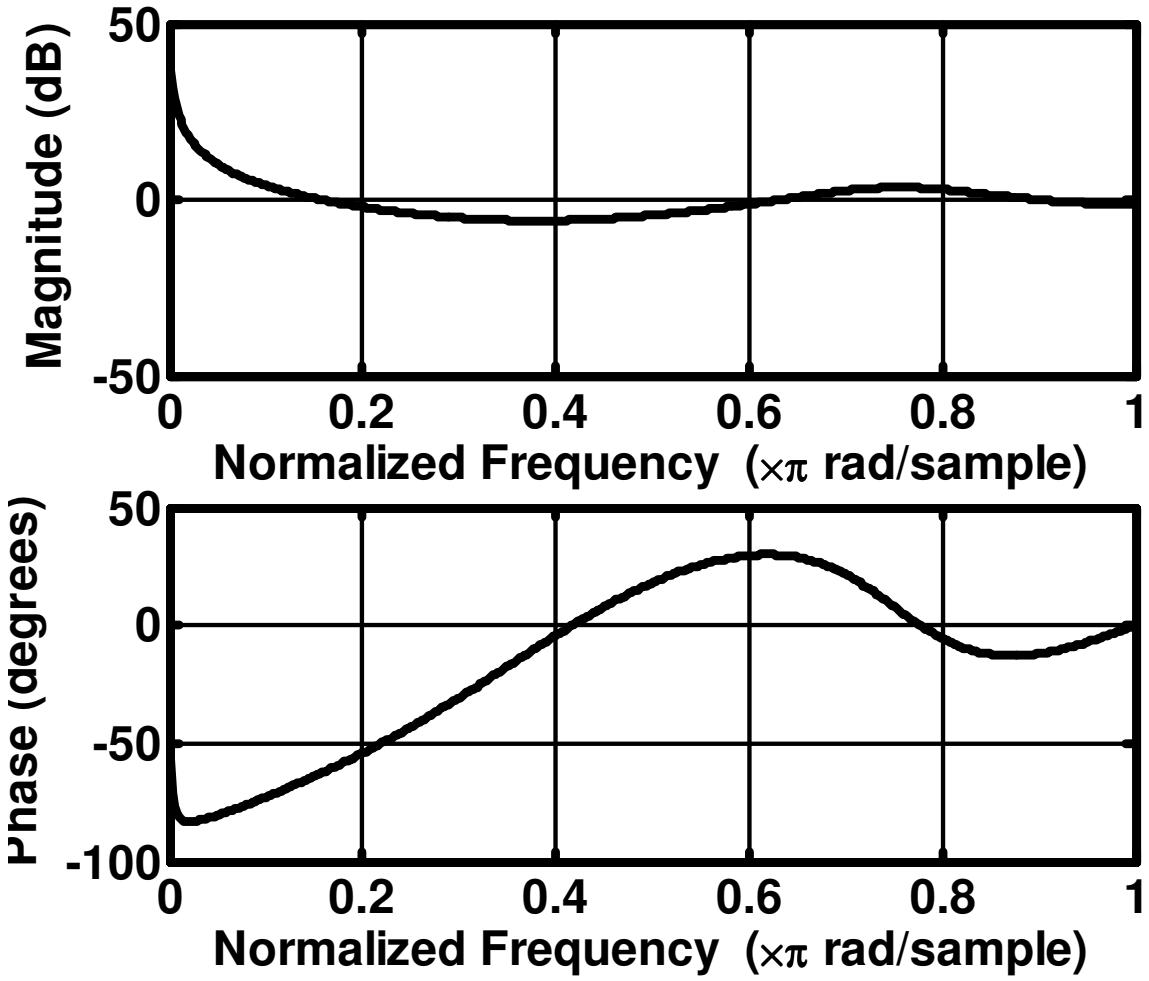
Magnitude (dB)
50
0
-50
0
0.2
0.4
0.6
0.8
1
Normalized Frequency (×π rad/sample)
Phase (degrees)
50
0
-50
-100
0
0.2
0.4
0.6
0.8
1
Normalized Frequency (×π rad/sample)

Figure 9

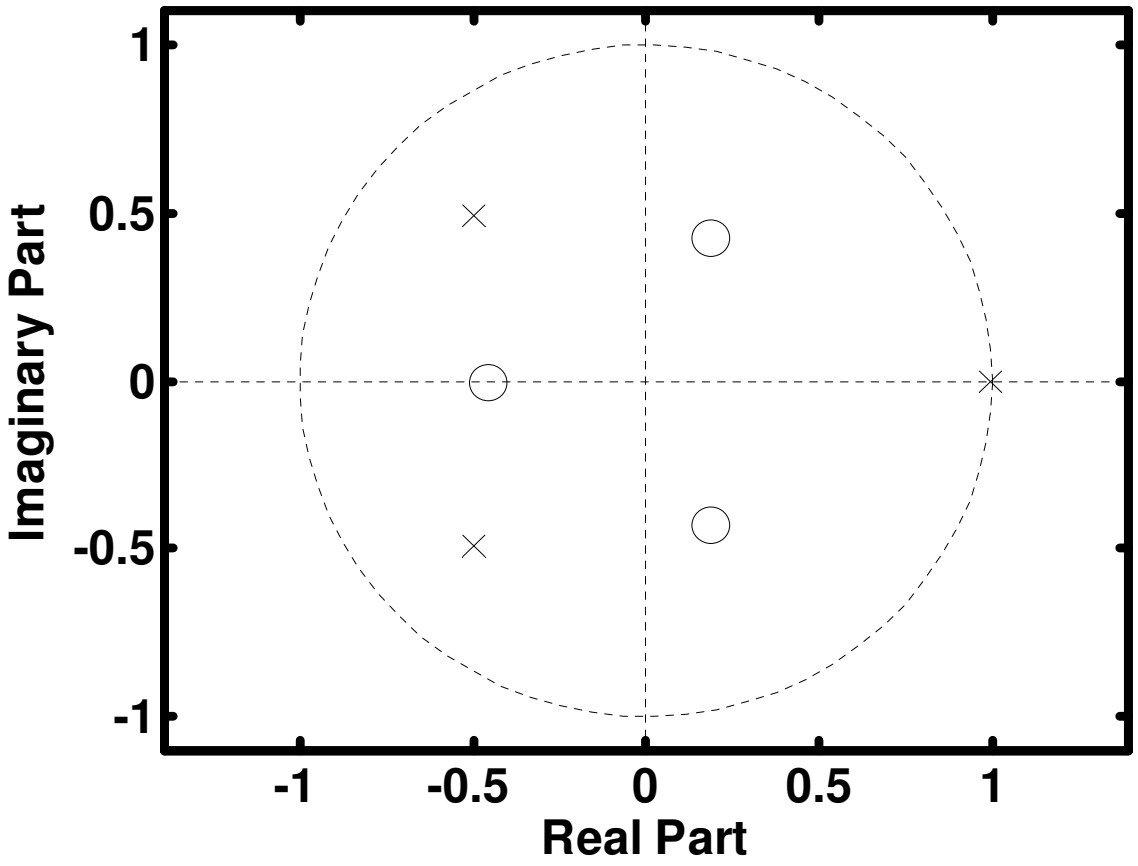

Table 1

All-zero system			
G0,1 = 1.414	G1,0 = 1.414 X b0	G2,1 = 1.414	G3,0 = 1.414
G0,3 = 1.414	G1,2 = 1.414 X b1	G2,3 = 1.414	
G0,5 = 1.414	G1,4 = 1.414 X b2	G2,5 = 1.414	
	G1,6 = 1.414 X b3		
All-pole system			
G4,1 = 1.414	G5,0 = 1.414	G6,1 = 1.414	G7,0 = 1.414
G4,3 = 1.414	G5,2 = 1.414 X (- a2)	G6,3 = 1.414	
	G5,4 = 1.414 X (- a3)		

Table 2

All-zero system			
G0,1 = 1.414	G1,0 = 1.414	G2,1 = 1.414	G3,0 = 1.414
G0,3 = 1.414	G1,2 = 0.1414	G2,3 = 1.414	
G0,5 = 1.414	G1,4 = 0.0707	G2,5 = 1.414	
	G1,6 = 0.1414		
All-pole system			
G4,1 = 1.414	G5,0 = 1.414	G6,1 = 1.414	G7,0 = 1.414
G4,3 = 1.414	G5,2 = 0.707	G6,3 = 1.414	
	G5,4 = 0.6929		